The Intrinsic Frequency Response of 1.3-μm InGaAsN Lasers in the Range $T = 10$ °C–80 °C

O. Anton, L. F. Xu, D. Patel, C. S. Menoni, J. Y. Yeh, T. T. Van Roy, L. J. Mawst, and N. Tansu

***Abstract*—Optical modulation response experiments above threshold are carried out in ridge waveguide InGaAs and InGaAsN ($N = 0.5\%$) in a temperature span of 10 °C–80 °C. The modulation traces are analyzed with a complete rate equation model that allows extraction of the resonance frequency and damping that are intrinsic to the carrier and photon processes occurring in the laser active region. This analysis enables calculation of the K-factor and its temperature behavior. K-values for InGaAsN lasers are larger and show a more pronounced dependence on temperature than in InGaAs lasers. This behavior is ascribed to a decrease in the effective differential gain with nitrogen content.**

***Index Terms*—3-dB bandwidth, InGaAsN quantum-well (QW) lasers, modulation response.**

I. Introduction

FIRST pioneered by Kondow [1], InGaAsN alloys have enabled the growth of 1.3-μm quantum wells (QWs) on GaAs, making possible vertical-cavity surface-emitting laser (VCSEL) fabrication on GaAs with speed performance characteristics suited for metropolitan area networks and optical interconnects. Benchmarks in terms of high-speed operation of 13.8-GHz modulation bandwidth [2] in multiple QW edge emitting devices have been demonstrated. However, there may be still room for improvement in terms of modulation bandwidth. Theoretical predictions have suggested dilute nitrides could reach frequency bandwidths of about 37 GHz at 27 °C and 18 GHz at 100 °C [3].

Motivated by the necessity to understand the processes that influence the frequency bandwidth of 1.3-μm InGaAsN QW lasers, we have investigated their intrinsic frequency response in a temperature range of 10 °C–80 °C. To isolate the role of nitrogen, the modulation responses of two identical laser structures that only differ in the nitrogen content in the well were contrasted. The effects of the device structure on the modulation response were accounted for by using an optical modulation technique previously described [4] which when combined with a complete rate equation model that includes the device parasitics [5] allowed extraction of a resonance frequency f_r and damping γ that are intrinsic to the carrier and photon processes in the laser active region.

Manuscript received March 22, 2006; revised June 5, 2006. This work was supported by NSF Grant ECS 03134410. The work of O. Anton was supported by the Agilent Photonics Fellowship, Agilent Technologies, Palo Alto, CA.

O. Anton, L. F. Xu, D. Patel, and C. S. Menoni are with the Department of Electrical and Computer Engineering, Colorado State University, Fort Collins, CO 80523-1373 USA (e-mail: carmen@engr.colostate.edu).

J. Y. Yeh, T. T. Van Roy, and L. J. Mawst are with the Reed Center for Photonics, Department of Electrical Computer Engineering, University of Wisconsin-Madison, Madison, WI 53706-1691 USA.

N. Tansu is with the Center for Optical Technologies, Department of Electrical and Computer Engineering, Lehigh University, Sinclair Laboratory, Bethlehem, PA 18015 USA.

Digital Object Identifier 10.1109/LPT.2006.880701

II. Experiments

Frequency response measurements by terahertz optical injection [4] were conducted on two identical $In_{0.4}Ga_{0.6}As$ and $In_{0.4}Ga_{0.6}As_{0.995}N_{0.005}$ single QW (SQW) lasers. The two device structures, grown by metal–organic chemical vapor deposition [6], consist of an SQW of width $L_w = 60$ Å surrounded by two tensile strain $GaAs_{0.85}P_{0.15}$ barriers, a 3000-Å GaAs separate confinement heterostructure region, and AlGaAs claddings. The uncoated InGaAsN (InGaAs) ridge waveguide (RWG) devices feature a stripe width of 3.5 μm and length 500 μm, with emission wavelengths of $\lambda = 1.3$ μm (1.2 μm). The lasers were biased by current pulses of 10-μs width and duty cycle $D < 10\%$ from one to four times the threshold current which for InGaAsN (InGaAs) devices varied between 11 and 30 mA (8 and 17 mA). The lasers were mounted in a baseplate whose temperature (T_b) was set to 10 °C, 20 °C, 40 °C, 60 °C, and 80 °C (± 1°C). The temperature of the active region was determined from the shift in wavelength of a longitudinal mode in the cavity using an optical spectrum analyzer. This method provides the average temperature increase within the 10-μs pulsewidth. The active area temperature differed from T_b by +1 °C up to 40 °C and by +2 °C above. As these temperature increments are not significant, we choose T_b to benchmark the high-frequency behavior of the InGaAsN(InGaAs) laser diodes.

For the frequency response measurements, the optical modulation was realized by injecting a train of <1-ps pulses and a wavelength of $\lambda \approx 1070$ nm ($\Delta\lambda \leq 20$ nm), and 12.5-ns repetition rate into the rear facet of the test laser [4]. The frequency response was acquired by collecting the output from the laser's front facet with a 12-GHz New Focus 1567 photodetector (PD). The output signal from the PD was measured with a Agilent 8593 spectrum analyzer with a frequency span ranging from 70 MHz to 12 GHz. The frequency responses were obtained during the 10-μs span of the bias pulsewidth by gating the spectrum analyzer. The intermediate frequency bandwidth of the instrument was set to 100 KHz. This pulsed-bias method to measure the frequency responses allowed us to operate the lasers at significantly high biases with minimum active area heating.

III. Results and Analysis

Fig. 1 shows the frequency response traces obtained in InGaAsN and InGaAs lasers at a per facet emission power $P_0 = 3$ mW at $T_b = 10$ °C (top) and $T_b = 80$ °C (bottom). These traces are contrasted with electrical modulation responses to emphasize the advantages of the optical modulation scheme in

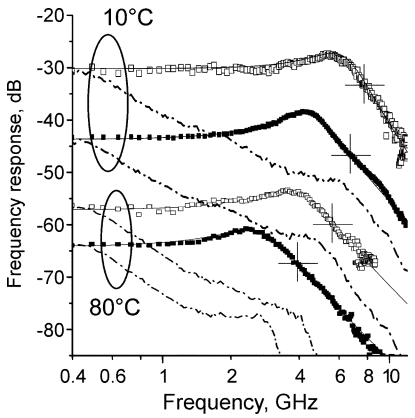

Fig. 1. Frequency responses obtained in InGaAsN (solid squares) and InGaAs (open squares) RWG SQW laser diodes at $P_0 = 3$ mW and $T_b = 10$ °C and 80 °C. Their −3-dB frequency is identified by the crossed lines. Electrical modulation traces are shown by the dashed–dotted lines.

minimizing the effect of the device parasitics on the modulation response. The solid lines are fits performed with a transfer function of resonance frequency f_r and damping λ that is solution to a rate equation analysis and that includes the effects of the electrical circuitry and oxide and $p-n$ junction capacitances [5]. The influence of the transport pole τ_c in the modulation traces is negligible satisfying the condition $1/\tau_c > 2\pi f_r$ for all output powers and temperatures.

Considering that the RWG lasers were optimized for low threshold current, and not specifically for high-frequency operation, the SQW InGaAsN (InGaAs) reach a −3-dB frequency of 6.7 GHz (8.1 GHz) at moderate $P_0 = 3$ mW at $T = 10$ °C. The traces of Fig. 1 also show that at the same per-facet output power and across the whole temperature range, InGaAsN lasers are characterized by a lower −3-dB bandwidth.

The parameters f_r and γ for InGaAsN and InGaAs lasers at all biases and temperatures, are plotted in Fig. 2. Fig. 2(a) shows f_r^2 versus emitted power P_o at different temperatures in InGaAsN and InGaAs lasers. The traces follow a linear behavior with P_o, indicating that gain compression is negligible. Fig. 2(a) also shows that the reduction in the $f_r^2 - P_o$ slope with temperature is more significant in InGaAsN lasers.

In the analysis of the damping γ versus P_o and temperature, the rate equation model was used to remove from γ the contributions from the laser parasitics. This correction is insignificant in InGaAsN but not in InGaAs lasers due to their larger $(\times 2)$ dynamic diode resistance [5]. A similar correction in f_r is not necessary as shown previously [5]. The corrected γ is plotted with respect to f_r^2 in Fig. 2(b). These traces show that γ is larger and more temperature-sensitive in InGaAsN than in InGaAs RWG lasers.

The experimental data of Fig. 2 was analyzed to extract the K-factor, $K = 2\pi(d\gamma/df_r^2)$, used to benchmark the high-speed response of laser diodes. K, obtained from the slope of the $\gamma - f_r^2$ trace, reflects the intrinsic carrier and photon dynamic processes that occur in the laser active region. Furthermore, the differences in K between the two identical InGaAsN and InGaAs RWG lasers can solely be ascribed to the incorporation of nitrogen in the active region SQW. Fig. 3(a) shows K in the

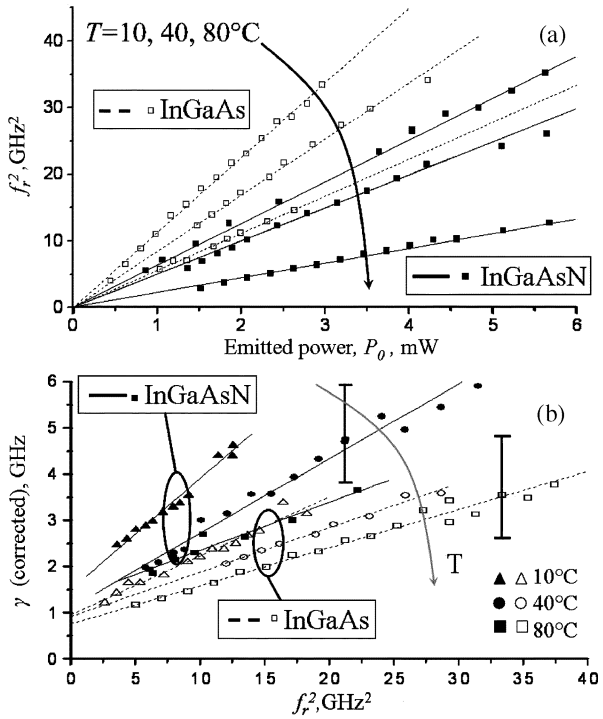

Fig. 2. (a) Resonance frequency squared, f_r^2 versus emitted power P_0 and (b) damping λ versus f_r^2 obtained in InGaAsN (solid symbols) and InGaAs (open symbols) RWG SQW laser diodes at $T_b = 10, 40$ °C, and 80 °C.

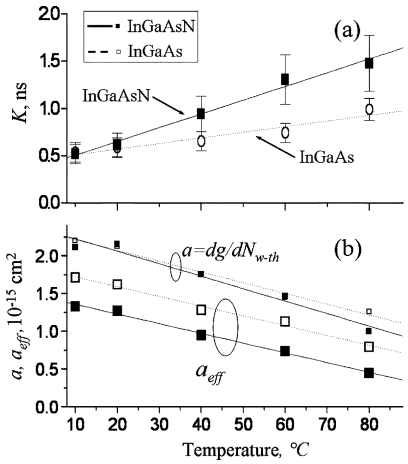

Fig. 3. (a) K-factor and (b) effective differential gain $a_{\rm eff}$, T_b in InGaAsN (solid squares) and InGaAs (open squares) RWG SQW laser diodes at $T = 10$ °C, 40 °C, and 80 °C. The smaller symbols and gray solid and dotted lines correspond to $dg/dN_{\rm w-th}$, obtained assuming $\tau_{\rm cap}$ and $\tau_{\rm esc}$ as given in the text.

range $T_b = 10$ °C–80 °C for InGaAsN and InGaAs RWG lasers. In InGaAsN lasers, K triples when T_b rises from 10 °C to 80 °C, while in InGaAs devices, K increases by about a factor of 2. The differences in the behavior of K, with and without nitrogen and with temperature, can be accounted for by the changes in the effective differential gain $a_{\rm eff}$. For a laser diode's response not limited by the carrier transport pole as in our devices, K is expressed in terms of the threshold material's differential gain $(dg/dN_{\rm w-th})$, the ratio of carrier capture $(\tau_{\rm cap})$ to escape $(\tau_{\rm esc})$

times, the gain compression factor (ε), and the photon density in the cavity (N_{po}) [7] as

$$a_{\rm eff} = \frac{dg/dN_{\rm w-th}}{(1+\tau_{\rm cap}/\tau_{\rm esc})(1+\varepsilon N_{po})}. \quad (1)$$

$a_{\rm eff}$ was extracted from the slope of $f_r^2 - P_o$ in Fig. 2(a), while simultaneous fitting of K in Fig. 3(a) allowed extraction of ε which was found equal to $(1.3\pm0.3).10^{-17}$ cm^{-3} in both structures. Fig. 3(b) plots $a_{\rm eff}$ for InGaAs and InGaAsN lasers in the temperature range of 10 °C–80 °C. $a_{\rm eff}$ is lower for InGaAsN lasers and it decreases by a factor of $\sim \times 3$ ($\sim \times 2$) in InGaAsN (InGaAs) in the temperature range of 10 °C–80 °C. At $T_b = 10$ °C, the reduction in $a_{\rm eff}$ due to the 0.5% increase of nitrogen content is ~22%. A similar trend in $a_{\rm eff}$ was also determined from the room temperature relative intensity noise spectra of the same laser structures [8]. At $T_b = 80$ °C, the difference in $a_{\rm eff}$ between the nitrogen containing and nitrogen free laser structures reaches ~50%.

We can now speculate on the factors that affect $a_{\rm eff}$ and thus K. Within the framework of gain and carrier density clamped at threshold, and considering that $\varepsilon N_{po} \ll 1$ as supported by the linearity of the traces in Fig. 2(a), the decrease in $a_{\rm eff}$ can be accounted for by the decrease in the threshold differential gain $dg/dN_{\rm w-th}$ or by the increase in the threshold transport factor $(1+\tau_{\rm cap}/\tau_{\rm esc})$.

We considered first the case in which $a_{\rm eff}$ is completely dominated by $dg/dN_{\rm w-th}$, and set $\tau_{\rm cap}/\tau_{\rm esc} \rightarrow 0$. In this limit, $dg/dN_{\rm w-th}$ tracks $a_{\rm eff}$ in Fig. 3(b), reducing by ~22% with 0.5% nitrogen content and by $\sim \times 3$ ($\sim \times 2$) for InGaAsN (InGaAs) as T_b decreases from 10 °C to 80 °C. A decrease in $dg/dN_{\rm w-th}$ with nitrogen content has been predicted by model calculations. There are, however, discrepancies in the magnitude of this decrease. Tomic *et al.* calculates a ~25% decrease in $dg/dN_{\rm w-th}$ with 0.5% addition of nitrogen [9] while Ng *et al.* [10] model predicts a 5%–7% decrease. The temperature behavior of $dg/dN_{\rm w-th}$ is well explained by the temperature variation of the bandgap and Fermi functions.

To evaluate the contribution of the transport factor, we calculated $\tau_{\rm cap}$ and $\tau_{\rm esc}$ in the InGaAsN and InGaAs QW for carrier densities of $\sim 3-4\cdot10^{18}$ cm^{-3} in the temperature range $T_b = 10$ °C–80 °C, as done in [11]. By letting $(1+\tau_{\rm cap}/\tau_{\rm esc})^{-1}$ vary between 0.63–0.45 (0.78–0.63) for InGaAsN (InGaAs), $dg/dN_{\rm w-th}$ was extracted from the data of Fig. 3(b). The results of this analysis, shown also in Fig. 3(b), yield $dg/dN_{\rm w-th}$ equal to $\sim 2.2\times10^{15}$ cm^{-2} at 10 °C and with almost identical temperature behavior in both materials. This scenario of a stronger contribution from carrier transport is supported by analysis of spontaneous emission spectra on identical laser structures that have suggested $dg/dN_{\rm w-th}$ is very similar between the nitrogen free and nitrogen containing materials [12]. A separate analysis of the injection efficiency in InGaAsN and InGaAs QW laser structures designed to enhance the effects of carrier transport have also assessed the more significant contribution of hole thermonic escape in the dilute nitrides [13].

IV. Summary

The optical modulation responses of two identical SQW RWG lasers with 0.5% and 0% nitrogen content in the well have been measured over a wide range of output powers in the temperature range of 10 °C–80 °C. Analysis of optical modulation responses with a simulation that removes the influence of the device parasitics, allows extraction of the resonance frequency and damping. The former is found to decrease and the latter to increase when the nitrogen content in the QW increases. Furthermore, both of these parameters are found to be more highly temperature-sensitive in InGaAsN. This behavior is ascribed to the reduction of the threshold effective differential gain ($a_{\rm eff}$) that contains the contributions from the QWs differential gain and the effective QW carrier capture and escape processes. The effective differential gain ($a_{\rm eff}$) is ~22% lower in InGaAsN at 10 °C and reduces by a factor of $\times 3$ ($\times 2$) in InGaAsN (InGaAs) at 80 °C.

It is important to note that a large fraction of the changes in $a_{\rm eff}$ may be accounted for the transport effect which is more significant in InGaAsN QW. Thus, optimizing the heterostructure of InGaAsN QW lasers for minimizing the transport effect is crucial to significantly improve the modulation response of the lasers at room and elevated temperatures.

References

[1] M. Kondow, S. Nakatsuka, T. Kitatani, Y. Yazawa, and M. Okai, "Room-temperature pulsed operation of GaInNAs laser diodes with excellent high-temperature performance," *Jpn. J. Appl. Phys., Regular Papers Short Notes and Review Papers*, vol. 35, pt. 1, pp. 5711–5713, 1996.

[2] D. Gollub, S. Moses, and A. Forchel, "1.3 μm double quantum well GalnNAs distributed feedback laser diode with 13.8 GHz small signal modulation bandwidth," *Electron. Lett.*, vol. 40, pp. 1181–1182, 2004.

[3] J. C. L. Yong, J. M. Rorison, M. Othman, H. D. Sun, M. D. Dawson, and K. A. Williams, "Simulation of gain and modulation bandwidths of 1300 nm RWG InGaAsN lasers," in *Proc. Inst. Elect. Eng., Optoelectron.*, 2003, vol. 150, pp. 80–82.

[4] O. Anton, G. Vaschenko, D. Patel, G. Y. Robinson, C. S. Menoni, and J. Pikal, "Small signal response of 1.3 mm InAsP–InGaAsP quantum-well laser diodes obtained with a terahertz-bandwidth frequency comb," *IEEE J. Quantum Electron.*, vol. 40, no. 8, pp. 982–988, Aug. 2004.

[5] O. Anton, D. Patel, C. S. Menoni, J. Y. Yeh, T. T. Van Roy, L. Mawst, J. Pikal, and N. Tansu, "Frequency response of strain-compensated InGaAsN-GaAsP-GaAs SQW lasers," *IEEE J. Sel. Topics Quantum Electron.*, vol. 11, no. 5, pp. 1079–1088, Sep./Oct. 2005.

[6] N. Tansu, J. Y. Yeh, and L. J. Mawst, "Extremely-low threshold-current-density InGaAs quantum well lasers with emission wavelength of 1215–1233 nm," *Appl. Phys. Lett.*, vol. 82, pp. 4038–4040, Jun. 2003.

[7] L. A. Coldren and S. W. Corzine, *Diode Lasers and Photonic Integrated Circuits*, ser. Wiley Series in Microwave and Optical Engineering. New York: Wiley, 1995.

[8] L. Shterengas, G. Belenky, J. Y. Yeh, L. J. Mawst, and N. Tansu, "Differential gain and linewidth enhancement factor in dilute-nitride GaAs-based 1.3 mm diode lasers," *IEEE J. Sel. Topics Quantum Electron.*, vol. 11, no. 5, pp. 1063–1068, Sep./Oct. 2005.

[9] S. Tomic, E. P. O'Reilly, S. J. Sweeney, A. R. Adams, A. D. Andreev, S. A. Choulis, T. J. C. Hosea, and H. Riechert, "Theoretical and experimental analysis of 1.3- μm InGaAsN/GaAs lasers," *IEEE J. Sel. Topics Quantum Electron.*, vol. 9, no. 5, pp. 1228–1238, Sep./Oct. 2003.

[10] S. T. Ng, W. J. Fan, Y. X. Dang, and S. F. Yoon, "Comparison of electronic band structure and optical transparency conditions of $In_xGa_{1x}As_{1y}N_y$/GaAs quantum wells calculated by 10-band, 8-band, and 6-band $k\cdot p$ models," *Phys. Rev. B*, vol. 72, no. 11, 2005, article no. 115341.

[11] N. Tansu and L. J. Mawst, "The role of hole leakage in 1300-nm InGaAsN quantum-well lasers," *Appl. Phys. Lett.*, vol. 82, pp. 1500–1502, 2003.

[12] D. J. Palmer, P. M. Smowton, P. Blood, J. Y. Yeh, L. J. Mawst, and N. Tansu, "Effect of nitrogen on gain and efficiency in InGaAsN quantum-well lasers," *Appl. Phys. Lett.*, vol. 86, no. 7, 2005, article no. 071121.

[13] J. Y. Yeh, L. J. Mawst, and N. Tansu, "The role of carrier transport on the current injection efficiency of InGaAsN quantum-well lasers," *IEEE Photon. Technol. Lett.*, vol. 17, no. 9, pp. 1779–1881, Sep. 2005.